Molecular approaches to uncover phage-lactic acid bacteria interactions in a model community simulating fermented beverages

Pierre Ledormand, Nathalie Desmasures, Benoit Bernay, Didier Goux, Oliver Rué, Cédric Midoux, Christophe Monnet, Marion Dalmasso

Molecular approaches to uncover phage-lactic acid bacteria interactions in a model community simulating fermented beverages.

Pierre Ledormand[1], Nathalie Desmasures[1], Benoit Bernay[2], Didier Goux[3], Oliver Rué[4 5], Cédric Midoux[4 5 6], Christophe Monnet[7], Marion Dalmasso[1]

[1] Normandie Univ, UNICAEN, UNIROUEN, ABTE, 14000, Caen, France

[2] Normandie Univ, UNICAEN, SFR ICORE, Proteogen Platform, 14000, Caen, France

[3] Normandie Univ, UNICAEN, SF ICORE 4206, CMAbio3, F-14032 Caen, France

[4] Université Paris-Saclay, INRAE, MaIAGE, 78350, Jouy-en-Josas, France

[5] Université Paris-Saclay, INRAE, BioinfOmics, MIGALE Bioinformatics Facility, 78350 Jouy-en-Josas, France

[6] Université Paris-Saclay, INRAE, PROSE, 92761 Antony, France

[7] Université Paris-Saclay, INRAE, AgroParisTech, UMR SayFood, 78850 Thiverval-Grignon, France

*Corresponding author:

Mailing address: EA 4651 ABTE, Esplanade de la Paix, 14032 Caen cedex 05, France

Phone: +33 (0)2 31 56 51 56

Fax: +33 (0)2 31 56 61 79

Email: marion.dalmasso@unicaen.fr

Abstract

Food microbial diversity and fluxes during the fermentation processes are well studied whereas phages-bacteria interactions are still poorly described in the literature. This is especially true in fermented beverages, and especially in cider, which is an alcoholic fermented apple beverage. The transcriptomic and proteomic responses of the lactic acid bacterium (LAB) *Liquorilactobacillus mali* UCMA 16447 to a lytic infection by phage UCMA 21115, both isolated from cider, were investigated, in order to get a better understanding of phages-bacteria interactions in such fermented beverage. During phage infection, 122 and 215 genes were differentially expressed in *L. mali* UCMA 16447 strain at T_{15} and T_{60} respectively, when compared to the uninfected condition. The same trends were confirmed by the proteomic study, with a total of 28 differentially expressed proteins found at T_{60}. Overall, genes encoding cellular functions, such as carbohydrate metabolism, translation, and signal transduction, were downregulated, while genes involved in nucleotide metabolism and in the control of DNA integrity were upregulated in response to phage infection. This work also highlighted that phage infection repressed many genes involved in bacterial cell motility, and affected glycolysis.

Keywords: Phage, fermented food, fermented beverage, microbial interactions, cider

1. Introduction

The diversity of bacteriophage (phage) communities, known as phageomes and to a larger extent as viromes, in fermented foods and beverages is poorly described, as reviewed by Ledormand et al., 2020. If the occurrence of phages in such environments has been demonstrated decades ago, the data which illustrate their impact on mixed communities and their ecological roles are scarce when compared to other microbial ecosystems (Paillet and Dugat-Bony, 2021). Phages are often studied for their negative impact on bacteria with technological interests like starter cultures, while they also play a major role as drivers of microbial communities (Mills et al., 2013). The behaviour of their bacterial hosts during phage infection has been reported in a few studies. This is especially true for a few potentially pathogenic bacteria such as *Pseudomonas aeruginosa* (Chevallereau et al., 2016; Lavigne et al., 2013; Zhao et al., 2016), *Yersinia enterocolitica* (Leskinen et al., 2016), and *Enterococcus faecalis* (Chatterjee et al., 2019), whose the transcriptomic response during phage infection was evaluated.

Lactic acid bacteria (LAB) are of great importance in the making and preservation of fermented foods and beverages. Knowledge about phages-LAB interactions remains to be developed. Some studies focusing on the response of the well-known dairy starter species *Lactococcus lactis* during phage infection have been carried out at the transcriptomic and the proteomic levels (Fallico et al., 2011; Ainsworth et al., 2013; Lemay et al., 2019, 2020). Apart from these data on *Lc. lactis*, little is known about the mechanisms of phages-LAB interactions in fermented foods and beverages. Cider, which is an alcoholic fermented apple beverage, is a typical example of a 'black box' ecosystem when it comes to phages-LAB interactions within the microbial communities throughout the fermentation process. Cider microbiota has the particularity to be less diverse than in other fermented foods, due to harsh physico-chemical conditions related in part to the low pH and the presence of ethanol (Misery

et al., 2021). Yeasts and LAB are the two types of microorganisms that contribute to the fermentation process of cider. Yeasts include *Saccharomyces* (*S. cerevisiae, S. uvarum)* and non-*Saccharomyces* (*Hanseniaspora*, *Candida*) genera, and are responsible for the alcoholic fermentation (Misery et al., 2021). The malolactic fermentation (MLF) is performed by LAB from *Oenococcus* sp., *Leuconostoc* sp., *Pediococcus* sp. and other *Lactobacillaceae* genera (members of the former *Lactobacillus* genus) (Cousin et al., 2017). Among these LAB, *Liquorilactobacillus mali* is a species which is commonly isolated from apple juice and cider. *L. mali* cells are Gram positive rods (0.6 µm × 1.8-4.2 µm), catalase positive, homofermentative, potential biogenic amine productive and motile (Carr and Davies, 1970; Coton et al., 2010; Cousin et al., 2015; Neville et al., 2012). To date no phage targeting *L. mali* is known.

More generally, the diversity of phages in cider has not been described yet, and much less how phage predation could influence cider fermentation (Ledormand et al. 2020). Deciphering the role of phages in cider microbial communities would contribute to get a better understanding of the microbial dynamics involved in fermentation processes. The aim of the present study was to assess the interactions between phage UCMA 21115 and its LAB host strain, *L. mali* UCMA 16447, both originating from cider, by means of transcriptomic and proteomic methods.

2. Materials & Methods

2.1 Bacterial strains and growth conditions

Five strains, *Liquorilactobacillus mali* UCMA 16447 strain, *L. mali* UCMA 19420 strain, *Secundilactobacillus collinoides* UCMA 16566 strain, *S. collinoides* UCMA 20009 strain, and *Lactobacillaceae sp. nov.* UCMA 15818 strain (unpublished data), were used in this study. They were from the UCMA collection (Université de Caen Microbiologie Alimentaire, Caen, France) and all originated from cider. Strains were routinely aerobically grown in de Man Rogosa & Sharpe (MRS; Difco) broth adjusted to pH 5.5, supplemented with 5 g/L of fructose and 0.5 g/L of cysteine, and incubated at 30°C for 24 hours.

2.2 Phage isolation, propagation and titration

Phage UCMA 21115 was isolated from a traditional French cider sample collected in the Normandy region (France). Its isolation and propagation were performed against the *L. mali* UCMA 16447 strain. Phage isolation was performed with an enrichment step where 1 mL of cider was added to a 10 mL-culture of *L. mali* UCMA 16447 at the exponential growth phase, and incubated overnight at 30°C. The phage enrichment in MRS medium was centrifuged at 4,700 × g for 20 min and filtered sterile using 0.45 µm filters, and stored at 4°C. Phage isolation and propagation were carried out using the classical double layer plate technique using MRS agar 0.5% (w/v) supplemented with 10 mM $CaCl_2$ and 10 mM $MgSO_4$, and incubated at 30°C for 24 h to allow the formation of plaques. Phage titration was expressed as plaque-forming units per mL (PFU/mL).

2.3 Electron microscopic analysis

Phage lysates (10^9 PFU/mL) were purified on a caesium chloride gradient by ultracentrifugation (Dalmasso et al., 2016). The phage phase was then collected and dialyzed

in phage buffer (100 mM Tris-HCl pH 7.5; 100 mM NaCl, 10 mM $MgCl_2$) overnight at 4°C. The phages were then observed with the transmission electron microscope JEOL 1011 (accelerating voltage of 80 kV), after a negative staining with uranyl acetate (1.5%).

2.4 Adsorption rate of phage UCMA 21115

Phage UCMA 21115 was added to *L. mali* UCMA 16447 at a multiplicity of infection (MOI) of 0.1 and incubated at 30°C for 30 min. Every 5 min, 2 mL were collected and filtered through a 0.45 um filter in order to assess the phage titer in the supernatant by counting the plaques using the double layer agar method. The adsorption rate was calculated with the formula $(N_0\text{-}N_t/N_0)*100$ where N_0 represents the phage titer used before the co-incubation, and N_t the phage titer at time t in the supernatant after filtration (Feng et al., 2020). The amount rate of non-adsorbed phages compared to the amount of phages for the infection is represented with the standard deviations of three independent experiments.

2.5 One-step-growth experiments (OSGC)

The OSCG was performed as described by Jaomanjaka et al., 2016, in triplicate. Briefly, the *L. mali* UCMA 16447 strain was cultured until an OD_{600nm} value of 0.2, and 1 mL was centrifuged at 10,000 × g for 2 min. The pellet was re-suspended in 1 mL of phage UCMA 21115 lysate in order to yield a MOI of 0.1, and was then incubated for 30 min at 30°C to allow phage adsorption. The sample was centrifuged at 10,000 × g for 2 min to eliminate unabsorbed phages. The pellet was then diluted (10^{-3}) in MRS broth and incubated at 30°C. Some samples were collected every 30 min, filtered sterile with 0.45 µm filters, and enumerated using the double layer plate count agar method. The burst size, the latency and rise phases of phage UCMA 21115 were estimated. The OSCG is presented with the standard deviations of three independent experiments.

2.6 DNA extraction, genome sequencing and genome analysis

Phage DNA was extracted as described by Dalmasso et al., (2012) after phage fraction recovering issued from an ultracentrifugation at 35,000 × g for 3 h on a caesium chloride gradient. Whole phage genome sequencing was performed on an Illumina sequencer producing paired-end reads 2 × 150 bases in length. Reads were assembled into a contig using Unicycler (Wick et al., 2017). An *in sillico* genome analysis was performed using RAST (Rapid Annotation using Subsystem Technology) for ORFs and putative proteins prediction (Aziz et al., 2008). The genome of phage UCMA 21115 is available under the accession number: ON117153.

2.7 Constitution of a LAB model community for studying phage-bacteria interactions

The five LAB strains were grown separately overnight in MRS broth at 30°C as precultures. One litre of fresh MRS broth was inoculated with 10 mL of each of the four strains making up the model community (i.e. UCMA 19420, UCMA 16566, UCMA 20009, and UCMA 15818 strains), and incubated at 30°C until an OD_{600nm} value of 0.2. In the same way, 500 ml of MRS broth were inoculated with 5 mL of *L. mali* UCMA 16447 strain as preculture. Once the *L. mali* UCMA 16447 culture had reached an $OD_{600\ nm}$ value of 0.2, it was divided into two fractions: one fraction was infected by phage UCMA 21115 at a MOI of 0.1, and the other was not infected, and used as a growth control. The two fractions were immediately placed into cellulose dialysis tubes (MWCO 12000 – 14000, ROTH) (Saraoui et al., 2013), and immersed into the growth medium inoculated with the synthetic bacterial community. Dialysis tubing was made to contain *L. mali* UCMA 16447 strain but allows the exchange of solutes with the synthetic bacterial community. Incubation was carried out at 30°C. The samples from the dialysis tubes were taken at 0, 15 and 60 min after phage infection corresponding to the early infection phase (10 and 30 mL for RNA and protein extractions, respectively). The cells were harvested by centrifugation at 4,700 × g for 10 min and cell pellets were stored at -80°C prior to RNA and protein extraction. Three independent

biological replicates per growth condition were performed, which represented a total of 15 samples (3 replicates at T0, 3 replicates at T15 with and without phages, and 3 replicates at T60 with and without phages). At T0 and T60, 30 mL of the model community were also sampled for protein extraction.

2.8 RNA extraction

The pellets were re-suspended in 500 µL of TE buffer (0.01M Tris pH 7.5; 0.01M EDTA) and the cells were lysed at 6,000 × g at 4°C with a Precellys® (Bertin Technologie, France) using a mix of glass beads (1.5 mm, Dutsher, France) and zirconium beads (0.5 and 0.1 mm, Dutsher, France). Total RNA extraction was performed with TRIzol Reagent (Fisher Scientific, Illkirch, France) and chloroform/isoamyl alcohol (24:1) (Sigma Aldrich, USA) separation. RNA was then purified using Direct-Zol RNA Miniprep (ZymoResaerch, Irvinie, CA, USA) according to the manufacturer's instructions, and RNA integrity was checked on a denaturing agarose gel as described by Aranda et al., 2012. RNA quantification and qualification was performed using a Nano TECAN spectrophotometer (Life Science, Switzerland).

2.9 cDNA synthesis, RNA-Seq, reads mapping and data analyses

rRNA depletion (Fastselect kit, Qiagen), cDNA library construction and RNA-Seq sequencing were carried out at Genewiz, Inc. facilities (South Plainfield, NJ, USA). RNA sequencing was performed on an Illumina sequencer, producing paired-end reads of 2x150 bases in length. In order to eliminate Illumina adaptors from sequencing, FastP processor (Chen et al., 2018) was used before checking the quality of sequencing data with FastQC v.0.11.8 (de Sena Brandine and Smith, 2019). The reads were mapped against the genome of *L. mali* UCMA 16447 (Bioproject PRJNA727965) strain using Bowtie 2 (Langmead and Salzberg, 2012) with a minimal fragment size of 50 pb and counted using HTSeq v.0.9.1

processor (Anders et al., 2015). Reads matching with coding DNA sequences (CDS) were retrieved from the raw data set for subsequent analyses. The data were filtered to eliminate the genes displaying an average of less than 10 reads per sample for all data (15 samples). The statistical analysis of RNA-Seq data was performed using SARTools DESeq2 tool v.1.7.3 (Varet et al., 2016) with default settings. Gene transcripts with an adjusted p-value ($p < 0.05$) and a fold change of ≥ 2 and ≤ -2 (in absolute values) were considered to be differentially expressed between different conditions. The functional annotation of the transcripts was done using the Kyoto Encyclopedia of Gene and Genomes (KEGG).

The RNA-Seq data used in this study are available in NCBI SRA repository, under the reference number PRJNA804221.

2.10 Protein extraction

The cell pellets were re-suspended in 2 mL of wash buffer (50 mM TrisHCl pH 8.0, 1 mM PMSF), lysed at 6,000 x g with a Precellys® (Bertin Technologie, France) using a mix of glass beads (1.5 mm) and zirconium beads (0.5 and 0.1 mm), and centrifuged at 10,000 × g for 10 min at 4°C. The supernatant was recovered and the proteins were subsequently precipitated with four volumes of precipitation buffer (80% of acetone, 20% of 50 mM TrisHCl pH 8.0), and incubated for 1h at -80°C, then overnight at -20°C. The tubes were centrifuged at 13,000 × g for 10 min at 4°C. The supernatant was removed, and the pellets were dried for 30 min under a chemical hood. Finally, the proteins were re-suspended in a protein buffer (50 mM TrisHCl pH 8.0, 5% glycerol,1 mM EDTA, 1 mM PMSF, 100 mM NaCl), and quantified using the Bradford method (Bradford, 1976). The proteins were prepared from three independent biological replicates.

2.11 Mass-spectrometry analysis

Protein preparation and nLCMS analysis were performed as previously described (Aubourg et al., 2020). Before post-process, the samples were analysed using the Preview software (ProteinMetrics) in order to estimate the quality of the tryptic digestion and predict any post-translational modifications. The result presented below, is used for the "bank research / identification" part. The fragmentation pattern was used to determine the sequence of the peptide. Database searching was performed using the Peaks X+ software. A homemade database composed of *L. mali* UCMA 16447, *L. mali* UCMA 19420, *S. collinoides* UCMA 16566, *S. collinoides* UCMA 20009 and strain UCMA 15818, was used. The variable modifications allowed were as follows: Nterm-acetylation, methionine oxidation, Deamidation (NQ). In addition, C-Propionoamide was set as fix modification. "Trypsin" was selected as Specific. Mass accuracy was set to 30 ppm and 0.05 Da for MS and MS/MS mode, respectively. The data were filtered according to a FDR of 1%.

2.13 Identification of differentially expressed proteins

To quantify the relative levels of protein abundance between the different groups, the samples were analysed using the label-free quantification feature of the PEAKS X+ software. The features of the same peptides from all replicates of each sample were aligned through the retention time alignment algorithms. The mass error tolerance was set at 30 ppm, Ion Mobility Tolerance (1/k0) at 0.05 and the retention time tolerance at 7 min. The normalization factors of the samples were obtained by the total ion current (TIC) of each sample. The quantification of the protein abundance level was calculated using the sum area of the top three unique peptides. A 1.5-fold increase in relative abundance and a Peak significance $\geq$ 15 using ANOVA as significance method were used to determine the enriched proteins.

225 # 3. Results

226 ### *3.1 Characterization of phage UCMA 21115*

227 Phage UCMA 21115 was isolated from a French cider sample, and infected *L. mali* UCMA
228 16447 strain. This phage has a small-isometric head and a long non-contractile tail, which
229 indicates that it belongs to the *Siphoviridae* family of the order Caudovirales (**Fig. 1**). The
230 head diameter was 60.18 nm ± 3 nm (n = 3) and the tail length was 223.68 nm ± 5 nm (n = 3).
231 The lytic activity of phage UCMA 21115 was assessed in MRS broth pH 5.5 at different MOI
232 values (1, 0.1 and 0.01) by performing OD_{600nm} measurements (**Fig. S1**). Phage UCMA 21115
233 lysed its hosts in 4 h at a MOI of 1. A lytic activity was observed up to a MOI of 0.01 (**Fig.**
234 **S1**). As it was isolated from cider, which is an acidic fermented beverage, phage UCMA
235 21115 was also checked for its ability to resist to acidic pH values ranging from pH 3.0 to pH
236 5.5 (**Fig. S2**). Phage UCMA 21115 showed a strong resistance at pH values above 4.0 (**Fig.**
237 **S2**). Phage UCMA 21115 targeted only *L. mali* UCMA 16447 strain among the 120 tested
238 LAB strains (including strains of *Leuconostoc* sp., *Oenococcus* sp., *Pediococcus* sp. and
239 *Lactobacillaceae* members of the former *Lactobacillus* genus) (data not shown).

240 ### *3.2 Kinetics profile of phage UCMA 21115*

241 To establish the binding affinity of phage UCMA 21115 to its host strain *L. mali* UCMA
242 16447, the phage adsorption to the bacterial cells was estimated during an incubation period
243 of 30 min. After 5 min, nearly 80% of the phage particles adsorbed to the bacterial cells (**Fig.**
244 **2A**). After 20 min, more than 95% of the phage particles were attached to the host cells.
245 To better understand the population dynamics of phage UCMA 21115, a one-step growth
246 curve (OSGC) experiment was performed in the presence of *L. mali* UCMA 16447 strain at a
247 MOI of 0.1. The latent period lasted approximatively 150 min, after 30 min of adsorption (T_0
248 is after 30 min of adsorption), before reaching the plateau phase after 240 min (**Fig. 2B**). The

burst size, which is the number of particles being released per cell, was of about 22 ± 2 phages produced per host cell.

3.3 Genome analysis of phage UCMA 21115

Phage UCMA 21115 has a genome of 27,915 bp with a G+C content of 36.3%. A total of 42 open reading frames (ORFs) were predicted from the genome with no tRNA found (**Table S1**). Among the 42 ORFs, 21 were predicted on the forward strand, 21 on the reverse orientation, and 7 out of the 42 ORFs were assigned to a predicted function by RAST. The strictly lytic activity was confirmed since no module associated with lysogeny was found inside the genome. The predicted functions found inside the genome were in relation to packaging (terminase subunit), replication (DNA polymerase subunit, DNA primase), structure protein (tail protein, phage protein) and lysis (hydrolase, lysin) (**Table S1**). The genome was also BLAST against the NCBI virus database to identify the most related phages. Phage UCMA 21115 was close to *Leuconostoc* phages, particularly phage P974 (accession number MN552147.1, identity = 99.65 %, coverage = 99%) and phage phiLNTR3 (accession number KC013029.1, identity = 99.45 %, coverage = 99%).

3.4 Global overview of the transcriptional response of L. mali UCMA 16447 when infected by phage UCMA 21115

In order to study the impact of the lytic phage UCMA 21115 on *L. mali* UCMA 16447 strain, a transcriptomic approach based on RNA-Seq was followed. As the first minutes after a stress are crucial for bacterial survival, three time points were chosen after phage infection: 0, 15 and 60 min (the adsorption time was not taken into account here). The gene levels of expression in cells subjected to phage infection were compared to uninfected cells.

About 115 millions of sequencing reads were generated for all conditions, and the number of reads per sample varied from 4.4×10^6 to 1×10^7 (**Fig. S3).**

273 Read counts were established for each CDS available on the reference genome. The threshold
274 for a comparative classification of gene expression was set to 2-fold with p <0.05 being
275 considered as a significant differentially expressed gene. This fold-change corresponds to a
276 change that is higher than 2 or lower than 0.5 in absolute values. **Table 1** presents the number
277 of up or down regulated genes for each comparison. When comparing the infected conditions
278 (P) to the control experiment, a total of 122 genes were differentially expressed (DE) after 15
279 min (T15 vs T15P). This number almost doubled after 60 min, with 215 DE genes (T60 vs
280 T60P). It appeared that translation, cell motility, signal transduction and carbohydrates
281 metabolism were the most affected KEGG functional categories of genes that were repressed
282 (**Fig. 3**). After 15 min of phage infection, 10, 8 and 7 genes involved in translation, cell
283 motility and signal transduction, respectively, were repressed (**Fig. 3A**). After 60 min of
284 infection, the same categories were affected, with an increase in the number of DE genes, and
285 especially in repressed genes. For example, 22 genes involved in cell motility, 22 involved in
286 translation, 15 involved in signal transduction and 15 involved in carbohydrates metabolism
287 were repressed (**Fig. 3B**). The number of induced genes after 60 min of infection increased in
288 the same functional categories than after 15 min, with 10 and 5 genes induced in the
289 nucleotide metabolism and in the carbohydrates metabolism, respectively (**Fig. 3B**). Three
290 genes involved in amino acid metabolism, replication and repair or folding, and sorting and
291 degradation were also induced (**Fig. 3B**).

292 ***3.5 Identification of the induced and repressed genes of L. mali UCMA 16447 during phage***
293 ***infection***

294 All the functions impacted by phage infection are depicted on **Fig. 4**.

295 *3.5.1 Drastic modifications of cell motility and chemotaxis during phage infection*

296 Cellular motility was one of the main repressed function during phage infection. After 60 min,
297 26 genes were repressed encoding proteins for flagellar assembly such as basal body
298 components (*fliE*; fold change of 0.46; *fliR;* fold change of 0.41), hook (f*lgB;* fold change of
299 0.29; *flgD;* fold change of 0.31), and filament (*fliS;* fold change of 0.13) (**Table S2**). In
300 addition to cell motility, 11 genes involved in chemotaxis belonging to the signal transduction
301 category were repressed. Among these genes involved in chemotaxis for the regulation of the
302 flagellar system, a methyl-accepting chemotaxis protein (MCP) (fold change of 0.15) and
303 genes encoding for two-component systems like *cheA*, *cheB* and *cheW* (fold change of 0.27;
304 0.17 and 0.18, respectively) were repressed (**Table S2**). Genes encoding in the stator of the
305 system (*MotA;* fold change of 0.13, and *MotB;* fold change of 0.18) were also repressed
306 (**Table S2**).

307 *3.5.2 Modification of the expression of translation-coding genes during phage infection*

308 The cellular translation was also repressed as evidenced by the downregulation of many of the
309 genes coding for ribosomal subunits. More than 20 of these genes were repressed after 60 min
310 of infection (fold change between 0.23 and 0.49) (**Table S2**). On the opposite, the genes
311 involved in the synthesis of amino acids like glycine, serine and threonine (homoserine
312 deshydrogenase; fold change of 2.11) (**Table S2**) were overexpressed during the infection.

313 *3.5.3 Large induction of functions for DNA replication during infection*

314 The machinery necessary for the replication and the synthesis of the phage genome was
315 induced. Genes encoding the biosynthesis of purines and pyrimidines were more expressed in
316 the infected condition than in the uninfected condition. For example, the ribonucleoside-
317 diphosphate reductase (*rNDP*; fold change of 3.82) and the orotidine-5'-phosphate
318 decarboxylase (*pyrF*; fold change of 2.07) genes were induced (**Table S2**). Genes coding for
319 enzymes essential to DNA replication, like DNA polymerase (*DNApol* subunit gamma; fold

change of 5.86) and DNA gyrase subunit A (*gyrA*; fold change 2.18) (**Table S2**), were overexpressed. Another gene coding for an enzyme which is probably involved in the recombination of DNA was also overexpressed (*RecR*; fold change of 3.12) (**Table S2**).

3.5.4 Inhibition of the glycolysis pathway during phage infection

Another gene functional class affected by phage infection was the metabolism of carbohydrates. The phosphotransferase system (PTS) involved in the mannose uptake was repressed during the infection (fold change of 0.40) (**Fig. 5** & **Table S2**). Several genes coding for enzymes involved in the Embden-Meyerhof pathway (glycolysis) were repressed (**Table S2**). It was the case for the phosphofructokinase gene (*pfk;* fold change of 0.42), the glyceraldehyde 3-phosphate dehydrogenase gene (*gpdh;* fold change of 0.43), the phosphoglycerate kinase gene (*pgk;* fold change of 0.38), the phosphoglycerate mutase gene (*pgm;* fold change of 0.49) and the triose phosphate isomerase gene (*tpi;* fold change of 0.42) (**Fig. 5**). Conversely, the D-lactate dehydrogenase coding gene (*ldh;* fold change of 2.52) was highly induced during phage infection (**Fig. 5**), suggesting an impact on the lactate metabolism. The overexpression of the fructose 1,6 biphosphatase coding gene (*fbp*; fold change of 3.99) (**Fig. 5**), which has an antagonistic activity to PFK, comes to reinforce the idea of an inhibition of the glycolysis pathway. Other genes encoding enzymes involved in carbohydrate metabolism were differentially expressed like the malate dehydrogenase gene (*mdh*; 2.80 fold) and the acetate kinase gene (*ack*; fold change of 0.47).

3.5.5 Other functions affected by phage infection

The genes involved in lipid metabolism, and more specifically in fatty acid biosynthesis, like the acetyl-CoA biotin carboxylase gene (*accC*; fold change of 0.32), the oxoacyl reductase gene (*fabG*; fold change of 0.35) and the hydroxyacyl dehydratase gene (*hcd*; fold change of 0.40) (**Table S2**) were repressed during phage infection.

Genes coding for membrane transporters like the ATP-binding cassette (ABC), the phosphate transport system ATP-binding protein (fold change of 0.46) and the energy transport system ATP-binding protein (fold change of 0.46) were downregulated, hence demonstrating a decline in nutrient uptakes from the cell environment (**Table S2**).

Genes encoding stress response proteins like chaperones GroES, GroEL (*groES*; *groEL*; fold change of 2.34 and 2.69, respectively) and DnaJ (*dnaJ*; fold change of 2.10) were induced during phage infection (**Table S2**). The largest group of induced genes encoded hypothetical proteins and proteins of unknown function.

As *L. mali* UCMA 16447 strain was part of a four-strain model community closely related at the genus level, the existence of possible signal exchanges during phage infection were also sought at the transcriptomic level in *L. mali* UCMA 16447 strain. No evidence of this phenomenon were found.

3.6 Changes in the proteome of L. mali UCMA 16447 strain during phage infection

In addition to the RNA-Seq analysis, a proteomic approach to identify the major proteins impacted by phage infection was carried out. Comparisons were made for *L. mali* UCMA 16447 strain between T0 and after 60 min with phage (T60P) and without phage (T60), and between T60 and T60P. It appeared that 229 proteins were differentially expressed between T0 and T60P (**Fig. S4**), and 227 of them were overexpressed at T60P. When comparing the proteomes at T60 and T60P (**Fig. 6**), 28 proteins were differentially expressed, and only one was under-expressed. The energy production and conversion category counted 5 DE proteins, followed by carbohydrate transport and metabolism, nucleotide transport and metabolism, and replication, recombination and repair, and translation (3 DE proteins for each category).

3.6.1 Confirmation of motility repression at the proteome level

The only protein that was less abundant during phage infection was the flagellin protein (fold change of -1.17) (**Table S3**). This observation followed the same pattern as RNA-Seq data analysis, indicating the repression of cell motility during phage infection.

3.6.2 Overproduction of DNA replication associated proteins during phage infection

An increase in purine biosynthesis-related proteins during phage infection was observed. For example, the hypoxanthine-guanine phosphoribosyltransferase (fold change of 1.48), an enzyme involved in this function was more present in the infected condition (**Table S3**). Proteins involved in nucleotide metabolism (D-amino acyl-tRNA deacylase, cytidylate kinase, and deoxyguanosine kinase; fold change of 1.69, 1.68 and 1.87, respectively) (**Table S3**) and in the replication and repair of DNA (DNA polymerase III, Sak2, and ribonucleoside diphosphate reductase; fold change of 1.65, 5.96 and 3.20, respectively) (**Table S3**) were more abundant in the infected condition than without phages, thus confirming the transcriptomic results.

3.6.3 Other proteins

Other DE proteins, especially the proteins involved in amino-acid transport and metabolism, were also identified. The tRNA adenine-methyltransferase, involved in amino acid biosynthesis, and a proline iminopeptidase, involved in the release of amino acids (fold change of 2.53 and 1.34, respectively) (**Table S3**), were more abundant in the phage infection condition than in the control condition. A universal stress protein not clearly identified was more abundant during phage infection than in the control condition (fold change of 1.77) (**Table S3**).

Overall, all these proteomic results followed similar patterns as the results obtained with the transcriptomic approach, with the exception of the L-2-hydroxyisocaproate dehydrogenase, that has a catalytic activity close to the phosphofructokinase and the triose phosphate

391 isomerase (fold change of 1.71 and 1.18, respectively) (**Table S3**). Indeed, these proteins
392 were more abundant with the proteomic approach whereas their encoding genes were
393 repressed with the transcriptomic method.
394 In parallel with these comparisons, a proteomic study was performed on the proteome of the
395 synthetic bacterial community, *i.e.* on *L. mali* UCMA 19420, *S. collinoides* UCMA 16566, *S.*
396 *collinoides* UCMA 20009 and *L.* sp. nov UCMA 15818. No differences were found between
397 the conditions with and without phages (data not shown).

4. Discussion

Exploring the response of a food bacterium to phage infection is essential to understand what happens at the population level, and more generally at the community level during fermentation processes. Phage-LAB interactions in fermented foods are poorly described using omics methods compared to phage-pathogenic bacteria interactions. In this context, phage UCMA 21115, the first lytic phage isolated from cider, was isolated and characterized. It targeted *L. mali* UCMA 16447 strain, also originating from cider. Phage UCMA 21115 belongs to the *Siphoviridae* family like other phages isolated from fermented foods and beverages. For example, phage Vinitor targeting *O. oeni* (Philippe et al., 2021), phage Φ1-A4 targeting *Ln.* mesenteroides (Lu et al., 2010), phage TP901-1 targeting *Lactococcus lactis* (Mahony et al., 2016) and phage ATCCB targeting *Levilactobacillus brevis* (Feyereisen et al., 2019) all belong to the *Siphoviridae* family. Phage UCMA 21115 has a genome of 27,915 bp, which is smaller than other *Lactobacillus Siphoviridae* like, for example, *L. plantarum* phage ATCC8014 displaying a 38,002 bp genome (Briggiler Marcó et al., 2019) and *L. delbrueckii* subsp. *bulgaricus* phage PMBT4 displaying a 31,399 bp genome (Sprotte et al., 2022). Phage UCMA 21115 was closer to *Leuconostoc* phages like phiLNTR3 (99.45 % of identity) isolated from dairy products, than to other *Lactobacillus* phages (Kot et al., 2014). The lytic potential of phage UCMA 21115 was characterized. The replication rate of a phage is proportional to the growth rate of the bacterial strain. Thus, cell lysis appears more or less quickly depending on the bacterial species and strain, and depending on the phage and its MOI. For example, it appeared after 24 hours for *O. oeni* IOEB S 277 strain during infection by phage Φ OE33PA (Jaomanjaka et al., 2016), and after 120 minutes for *Salmonella enterica* subsp. *enterica* serovar Enteritidis ATCC 13076 strain during infection by phage BPSELC-1 (Li et al., 2020). In the current study, the complete lysis *of L. mali* UCMA 16447 strain by phage UCMA 21115 occurred after 240 minutes.

Phage UCMA 21115 was then used in a model of infection of *L. mali* UCMA 16447 strain in order to comprehensively investigate the transcriptional and proteomic response of the host strain to phage infection, when placed within a bacterial community. To date, the classical approaches to investigate phage-host interactions, particularly using transcriptomic and proteomic methods, are based on single phage-strain couple models, as it was the case, for example, in the transcriptomic study of *Lc. lactis* UC509.9 strain and phages Tuc2009 and c2 (Ainsworth et al. 2013). In the current study, placing *L. mali* UCMA 16447 strain in dialysis tubing (Saraoui et al. 2013) immersed into a model community of four strains belonging to the *Lactobacillaceae* family was intended to create conditions that possibly favour interactions between strains. In artificial co-cultures, many positive interactions may occur, as reviewed by Canon et al., 2020. For example, co-cultivation promotes interactions like commensalism, cooperation, mutualism or syntrophy to enhance bacterial fitness or substrate utilization. In co-cultivation, a wide variety of molecules can be exchanged, like extracellular enzyme sharing, cross-feeding or quorum sensing signalling molecules. No differentially expressed proteins were found in the model community whether *L. mali* UCMA 16447 strain was infected or not. This may be the result of proteins being the last level of cell expression. Furthermore, the 60 minutes of the experiment may not be extended enough to observe significant differences in protein expression at the community level, if any. Studying the metatranscriptomic response of the community could be more informative in future works (Monnet et al., 2016).

The transcriptomic and proteomic results of *L. mali* UCMA 16447 response to phage infection tended to follow the same patterns with a few discrepancies that can be explained by the time span for protein expression regulation being longer than for transcription regulation. For example, more than 20 genes were downregulated in the cell motility functional category with RNA-Seq study whereas only two proteins were retrieved and differentially expressed

448 for this functional category with the proteomic approach. Such differences between
449 transcriptomic and proteomic results are often observed (Dalmasso et al., 2012).
450 As in other phage-bacteria transcriptomic studies, the current work showed that the genes
451 involved in DNA replication, transcription, nucleotide metabolism and amino acid biogenesis
452 were overexpressed to allow phage replication and virion synthesis (Ainsworth et al., 2013;
453 Danis-Wlodarczyk et al., 2018; Lavysh et al., 2017; Leskinen et al., 2016; Zhao et al., 2016).
454 Translation was another repressed function during phage infection, suggesting that phage
455 infection led to a decline in the translation of bacterial proteins. On the opposite, genes and
456 proteins involved in the metabolism of amino acids like glycine, serine and threonine were
457 overexpressed during the infection, presumably useful for the assembly of phage elements or
458 as an additional energy source. All these main metabolic functions are usually affected by
459 stress conditions as reported in other works, and especially for the members of the former
460 *Lactobacillus* genus (actual members of the *Lactobacillaceae* family) (Angelis et al., 2016).
461 The major overexpressed proteins during a phage infection globally belonged to categories
462 associated to DNA replication, nucleotide metabolism and the production of energy as has
463 been shown for *Salmonella* (Weintraub et al., 2019). In the present work, other DE proteins
464 involved in signal transduction and cell envelope were also found differentially expressed in a
465 study of *Lc. lactis* (Lemay et al., 2019). Namely, the proteins involved in the multiplication of
466 phage particles were retrieved as the most abundant ones.
467 The expression level of the genes involved in the carbohydrate metabolism was also modified
468 during the infection. The *pfk*, *gpdh*, *pgk* and *pgm* genes were repressed during infection, thus
469 suggesting an inhibition of the Embden-Meyerhof pathway (glycolysis) while the *ldh* gene
470 was overexpressed. The overexpression of the *ldh* gene was also observed during the phage
471 infection of a *Lc. lactis* strain, and the authors speculated that the NAD^+ formed during the
472 transformation of pyruvate to lactate served to the glycolysis pathway (Ainsworth et al.,

2013). Yet, in our study we showed that the glycolysis enzymes were repressed, and thus that glycolysis is likely to be severely impacted, and most probably slowed down. A previous work on a *Vibrio* phage showed that NAD^+ was necessary to phage DNA replication and that the phage had a pathway of NAD^+ salvage (Lee et al., 2017a). In the current work, it might put forward the hypothesis that a mechanism of inhibition of glycolysis combined with a high activity of the lactate dehydrogenase and malate dehydrogenase (during the conversion of oxaloacetate into malate) is triggered by phage UCMA 21115 in order to spare NAD^+, as has been described in another study conducted in *Vibrio* phages (Lee et al., 2017b).

Cell motility was another major function affected by phage infection in *L. mali* UCMA 16447 strain. Some genera and species belonging to the former *Lactobacillus* genus are motile, and *L. mali* is one of them (Cousin et al., 2015; Neville et al., 2012). The flagellar system of *L. mali* UCMA 16447 strain was repressed during the infection. Several assumptions can be made to explain this phenomenon, but remain speculative at this stage of the study. Some phage receptors are located on bacterial flagella, as has been shown in previous works on *Campylobacter jejuni* (Baldvinsson et al., 2014), *Salmonella* (Baldvinsson et al., 2014; Choi et al., 2013), and *Erwinia* phages (Evans et al., 2010). Some mechanisms may be triggered in *L. mali* UCMA 16447 strain to reduce flagella production to thwart the infection, if phage infection is related to the flagellum receptor in the current study. In the same way, it has been shown for *Agrobacterium* sp. (Gonzalez et al., 2018) that phage transfer to a receptor on the cell membrane requires motility. The repression of the motility system in *L. mali* UCMA 16447 strain could perhaps contribute to a defence-like mechanism to prevent or, at least, to slow down the infection, and thus to resist to phage attack. If the mechanisms that led to the down-regulation of the genes encoding motility are still unknown, it is also possible to assume that this phage-driven phenomenon helps the phage in save energy for its replication within its host. The flagellar system is energy-consuming and its down-regulation would consequently

be of benefit to the phage as suggested by a previous work where a similar regulation of the flagellar system was observed in *Bacillus thuringiensis* during phage infection (Wu et al., 2014).

5. Conclusion

In conclusion, this study made it possible to describe for the first time the transcriptomic and proteomic response of a LAB isolated from a fermented beverage (cider) to phage infection within a bacterial community model. This study has revealed a fairly large disturbance in the cell metabolism at the transcriptomic and proteomic levels, with specific responses to phage infection. Some impacts on the host response were observed in different functional categories like in cell motility and in the carbohydrate, amino acid and nucleotide metabolisms. Gaining knowledge of host response to phage infection is crucial to better understand and even control microbial equilibria throughout fermentation processes. A better understanding of phage-bacteria interactions in fermented foods is crucial in order to continue to providing consumers with sustainable products.

6. Acknowledgements

This work was supported by the French Ministère de l'Enseignement Supérieur, de la Recherche et de l'Innovation under a PhD Grant MENRT. The authors would like to thank all the lab members for helpful discussions, and particularly Prof Jean-Marie Laplace and Dr Marina Cretenet for the selection of the bacterial strains used in this study. We are grateful to the INRAE MIGALE bioinformatics facility (MIGALE, INRAE, 2020. Migale bioinformatics Facility, doi: 10.15454/1.5572390655343293E12) for providing computing and storage resources.

7. Disclosure statement

No potential conflict of interest was reported by the authors.

8. References

Ainsworth, S., Zomer, A., Mahony, J., Sinderen, D. van, 2013. Lytic Infection of *Lactococcus lactis* by Bacteriophages Tuc2009 and c2 Triggers Alternative Transcriptional Host Responses. Appl. Environ. Microbiol. 79, 4786–4798. https://doi.org/10.1128/AEM.01197-13

Anders, S., Pyl, P.T., Huber, W., 2015. HTSeq--a Python framework to work with high-throughput sequencing data. Bioinforma. Oxf. Engl. 31, 166–169. https://doi.org/10.1093/bioinformatics/btu638

Angelis, M.D., Calasso, M., Cavallo, N., Cagno, R.D., Gobbetti, M., 2016. Functional proteomics within the genus Lactobacillus. PROTEOMICS 16, 946–962. https://doi.org/10.1002/pmic.201500117

Aranda, P.S., LaJoie, D.M., Jorcyk, C.L., 2012. Bleach gel: A simple agarose gel for analyzing RNA quality. ELECTROPHORESIS 33, 366–369. https://doi.org/10.1002/elps.201100335

Aubourg, M., Dhalluin, A., Gravey, F., Pottier, M., Thomy, N., Bernay, B., Goux, D., Martineau, M., Giard, J.-C., 2020. Phenotypic and proteomic approaches of the response to iron-limited condition in *Staphylococcus lugdunensis*. BMC Microbiol. 20, 328. https://doi.org/10.1186/s12866-020-02016-x

Aziz, R.K., Bartels, D., Best, A.A., DeJongh, M., Disz, T., Edwards, R.A., Formsma, K., Gerdes, S., Glass, E.M., Kubal, M., Meyer, F., Olsen, G.J., Olson, R., Osterman, A.L., Overbeek, R.A., McNeil, L.K., Paarmann, D., Paczian, T., Parrello, B., Pusch, G.D., Reich, C., Stevens, R., Vassieva, O., Vonstein, V., Wilke, A., Zagnitko, O., 2008. The RAST Server: rapid annotations using subsystems technology. BMC Genomics 9, 75. https://doi.org/10.1186/1471-2164-9-75

548 Baldvinsson, S.B., Sørensen, M.C.H., Vegge, C.S., Clokie, M.R.J., Brøndsted, L., 2014.
549 *Campylobacter jejuni* Motility Is Required for Infection of the Flagellotropic
550 Bacteriophage F341. Appl. Environ. Microbiol. 80, 7096–7106.
551 https://doi.org/10.1128/AEM.02057-14
552 Bradford, M.M., 1976. A rapid and sensitive method for the quantitation of microgram
553 quantities of protein utilizing the principle of protein-dye binding. Anal. Biochem. 72,
554 248–254. https://doi.org/10.1016/0003-2697(76)90527-3
555 Briggiler Marcó, M.B., Quiberoni, A., Suárez, V., 2019. Virulence of *Leuconostoc* phages:
556 Influence of stress conditions associated to dairy processes on their host-phage
557 interactions. Int. J. Food Microbiol. 303, 26–31.
558 https://doi.org/10.1016/j.ijfoodmicro.2019.05.008
559 Canon, F., Nidelet, T., Guédon, E., Thierry, A., Gagnaire, V., 2020. Understanding the
560 Mechanisms of Positive Microbial Interactions That Benefit Lactic Acid Bacteria Co-
561 cultures. Front. Microbiol. 0. https://doi.org/10.3389/fmicb.2020.02088
562 Carr, J.G., Davies, P.A., 1970. Homofermentative *Lactobacilli* of Ciders including
563 *Lactobacillus mali* nov. spec. J. Appl. Bacteriol. 33, 768–774.
564 https://doi.org/10.1111/j.1365-2672.1970.tb02261.x
565 Chatterjee, A., Willett, J., Nguyen, U.T., Monogue, B., Palmer, K.L., Dunny, G.M., Duerkop,
566 B.A., 2019. Parallel genomics uncover novel enterococcal-bacteriophage interactions.
567 bioRxiv 858506. https://doi.org/10.1128/mBio.03120-19
568 Chen, S., Zhou, Y., Chen, Y., Gu, J., 2018. fastp: an ultra-fast all-in-one FASTQ
569 preprocessor. Bioinforma. Oxf. Engl. 34, i884–i890.
570 https://doi.org/10.1093/bioinformatics/bty560
571 Chevallereau, A., Blasdel, B.G., Smet, J.D., Monot, M., Zimmermann, M., Kogadeeva, M.,
572 Sauer, U., Jorth, P., Whiteley, M., Debarbieux, L., Lavigne, R., 2016. Next-Generation

573 "-omics" Approaches Reveal a Massive Alteration of Host RNA Metabolism during
574 Bacteriophage Infection of *Pseudomonas aeruginosa*. PLOS Genet. 12, e1006134.
575 https://doi.org/10.1371/journal.pgen.1006134
576 Choi, Y., Shin, H., Lee, J.-H., Ryu, S., 2013. Identification and Characterization of a Novel
577 Flagellum-Dependent *Salmonella*-Infecting Bacteriophage, iEPS5. Appl. Environ.
578 Microbiol. 79, 4829–4837. https://doi.org/10.1128/AEM.00706-13
579 Coton, M., Romano, A., Spano, G., Ziegler, K., Vetrana, C., Desmarais, C., Lonvaud-Funel,
580 A., Lucas, P., Coton, E., 2010. Occurrence of biogenic amine-forming lactic acid
581 bacteria in wine and cider. Food Microbiol. 27, 1078–1085.
582 https://doi.org/10.1016/j.fm.2010.07.012
583 Cousin, F.J., Le Guellec, R., Schlusselhuber, M., Dalmasso, M., Laplace, J.-M., Cretenet, M.,
584 2017. Microorganisms in Fermented Apple Beverages: Current Knowledge and Future
585 Directions. Microorganisms 5, 39. https://doi.org/10.3390/microorganisms5030039
586 Cousin, F.J., Lynch, S.M., Harris, H.M.B., McCann, A., Lynch, D.B., Neville, B.A., Irisawa,
587 T., Okada, S., Endo, A., O'Toole, P.W., 2015. Detection and Genomic
588 Characterization of Motility in *Lactobacillus curvatus* : Confirmation of Motility in a
589 Species outside the *Lactobacillus salivarius* Clade. Appl. Environ. Microbiol. 81,
590 1297–1308. https://doi.org/10.1128/AEM.03594-14
591 Dalmasso, M., Aubert, J., Briard-Bion, V., Chuat, V., Deutsch, S.-M., Even, S., Falentin, H.,
592 Jan, G., Jardin, J., Maillard, M.-B., Parayre, S., Piot, M., Tanskanen, J., Thierry, A.,
593 2012. A Temporal -omic Study of *Propionibacterium freudenreichii* CIRM-BIA1T
594 Adaptation Strategies in Conditions Mimicking Cheese Ripening in the Cold. PLoS
595 ONE 7, e29083. https://doi.org/10.1371/journal.pone.0029083
596 Dalmasso, M., Strain, R., Neve, H., Franz, C.M.A.P., Cousin, F.J., Ross, R.P., Hill, C., 2016.
597 Three New *Escherichia coli* Phages from the Human Gut Show Promising Potential

for Phage Therapy. PLOS ONE 11, e0156773. https://doi.org/10.1371/journal.pone.0156773

Danis-Wlodarczyk, K., Blasdel, B.G., Jang, H.B., Vandenheuvel, D., Noben, J.-P., Drulis-Kawa, Z., Lavigne, R., 2018. Genomic, transcriptomic, and structural analysis of *Pseudomonas* virus PA5oct highlights the molecular complexity among Jumbo phages. bioRxiv 406421. https://doi.org/10.1101/406421

de Sena Brandine, G., Smith, A.D., 2019. Falco: high-speed FastQC emulation for quality control of sequencing data. F1000Research 8, 1874. https://doi.org/10.12688/f1000research.21142.2

Evans, T.J., Trauner, A., Komitopoulou, E., Salmond, G.P.C., 2010. Exploitation of a new flagellatropic phage of *Erwinia* for positive selection of bacterial mutants attenuated in plant virulence: towards phage therapy. J. Appl. Microbiol. 108, 676–685. https://doi.org/10.1111/j.1365-2672.2009.04462.x

Fallico, V., Ross, R.P., Fitzgerald, G.F., McAuliffe, O., 2011. Genetic Response to Bacteriophage Infection in *Lactococcus lactis* Reveals a Four-Strand Approach Involving Induction of Membrane Stress Proteins, d-Alanylation of the Cell Wall, Maintenance of Proton Motive Force, and Energy Conservation. J. Virol. 85, 12032–12042. https://doi.org/10.1128/JVI.00275-11

Feng, T., Leptihn, S., Dong, K., Loh, B., Zhang, Y., Li, M., Guo, X., Cui, Z., 2020. Characterisation of bacteriophage JD419, a Staphylococcal phage with an unusual morphology and broad host range. bioRxiv 2020.11.09.370866. https://doi.org/10.1101/2020.11.09.370866

Feyereisen, M., Mahony, J., Lugli, G.A., Ventura, M., Neve, H., Franz, C.M., Noben, J.-P., O'Sullivan, T., Sinderen, D. van, 2019. Isolation and Characterization of *Lactobacillus brevis* Phages. Viruses 11, 393. https://doi.org/10.3390/v11050393

623 Gonzalez, F., Helm, R.F., Broadway, K.M., Scharf, B.E., 2018. More than Rotating Flagella:
624 Lipopolysaccharide as a Secondary Receptor for Flagellotropic Phage 7-7-1. J.
625 Bacteriol. 200. https://doi.org/10.1128/JB.00363-18
626 Jaomanjaka, F., Claisse, O., Blanche-Barbat, M., Petrel, M., Ballestra, P., Le Marrec, C.,
627 2016. Characterization of a new virulent phage infecting the lactic acid bacterium
628 *Oenococcus oeni*. Food Microbiol. 54, 167–177.
629 https://doi.org/10.1016/j.fm.2015.09.016
630 Kot, W., Neve, H., Heller, K.J., Vogensen, F.K., 2014. Bacteriophages of *Leuconostoc,*
631 *Oenococcus*, and *Weissella*. Front. Microbiol. 5.
632 https://doi.org/10.3389/fmicb.2014.00186
633 Lavigne, R., Lecoutere, E., Wagemans, J., Cenens, W., Aertsen, A., Schoofs, L., Landuyt, B.,
634 Paeshuyse, J., Scheer, M., Schobert, M., Ceyssens, P.-J., 2013. A Multifaceted Study
635 of *Pseudomonas aeruginosa* Shutdown by Virulent Podovirus LUZ19. mBio 4.
636 https://doi.org/10.1128/mBio.00061-13
637 Lavysh, D., Sokolova, M., Slashcheva, M., Förstner, K.U., Severinov, K., 2017. Transcription
638 Profiling of *Bacillus subtilis* Cells Infected with AR9, a Giant Phage Encoding Two
639 Multisubunit RNA Polymerases. mBio 8. https://doi.org/10.1128/mBio.02041-16
640 Ledormand, P., Desmasures, N., Dalmasso, M., 2020. Phage community involvement in
641 fermented beverages: an open door to technological advances? Crit. Rev. Food Sci.
642 Nutr. 1–10. https://doi.org/10.1080/10408398.2020.1790497
643 Lee, J.Y., Li, Z., Miller, E.S., 2017a. Vibrio Phage KVP40 Encodes a Functional NAD+
644 Salvage Pathway. J. Bacteriol. 199. https://doi.org/10.1128/JB.00855-16
645 Lee, J.Y., Li, Z., Miller, E.S., 2017b. Vibrio Phage KVP40 Encodes a Functional NAD+
646 Salvage Pathway. J. Bacteriol. 199. https://doi.org/10.1128/JB.00855-16

Lemay, M.-L., Maaß, S., Otto, A., Hamel, J., Plante, P.-L., Rousseau, G.M., Tremblay, D.M., Shi, R., Corbeil, J., Gagné, S.M., Becher, D., Moineau, S., 2020. A Lactococcal Phage Protein Promotes Viral Propagation and Alters the Host Proteomic Response During Infection. Viruses 12, 797. https://doi.org/10.3390/v12080797

Lemay, M.-L., Otto, A., Maaß, S., Plate, K., Becher, D., Moineau, S., 2019. Investigating *Lactococcus lactis* MG1363 Response to Phage p2 Infection at the Proteome Level*[S]. Mol. Cell. Proteomics 18, 704–714. https://doi.org/10.1074/mcp.RA118.001135

Leskinen, K., Blasdel, B., Lavigne, R., Skurnik, M., 2016. RNA-sequencing reveals the progression of phage-host interactions between φR1-37 and *Yersinia enterocolitica*. Viruses 8, 111. https://doi.org/10.3390/v8040111

Li, P., Xianjun, X., Xiuzhong Zhang, Tu, Z., Gu, J., Zhang, A., 2020. Characterization and Whole-Genome Sequencing of Broad-host-range *Salmonella*-specific Bacteriophages for Bio-control. Microb. Pathog. 104119. https://doi.org/10.1016/j.micpath.2020.104119

Lu, Z., Altermann, E., Breidt, F., Kozyavkin, S., 2010. Sequence Analysis of *Leuconostoc mesenteroides* Bacteriophage Φ1-A4 Isolated from an Industrial Vegetable Fermentation. Appl. Environ. Microbiol. 76, 1955–1966. https://doi.org/10.1128/AEM.02126-09

Mahony, J., Stockdale, S.R., Collins, B., Spinelli, S., Douillard, F.P., Cambillau, C., Sinderen, D. van, 2016. *Lactococcus lactis* phage TP901–1 as a model for *Siphoviridae* virion assembly. Bacteriophage 6, e1123795. https://doi.org/10.1080/21597081.2015.1123795

Mills, S., Shanahan, F., Stanton, C., Hill, C., Coffey, A., Ross, R.P., 2013. Movers and shakers: influence of bacteriophages in shaping the mammalian gut microbiota. Gut Microbes 4, 4–16. https://doi.org/10.4161/gmic.22371

Misery, B., Legendre, P., Rue, O., Bouchart, V., Guichard, H., Laplace, JM., Cretenet, M., 2021. Diversity and dynamics of bacterial and fungal communities in cider for distillation. Int. J. Food Microbiol. 339, 108987. https://doi.org/10.1016/j.ijfoodmicro.2020.108987

Monnet, C., Dugat-Bony, E., Swennen, D., Beckerich, J.-M., Irlinger, F., Fraud, S., Bonnarme, P., 2016. Investigation of the Activity of the Microorganisms in a Reblochon-Style Cheese by Metatranscriptomic Analysis. Front. Microbiol. 7. https://doi.org/10.3389/fmicb.2016.00536

Muller, C., Cacaci, M., Sauvageot, N., Sanguinetti, M., Rattei, T., Eder, T., Giard, J.-C., Kalinowski, J., Hain, T., Hartke, A., 2015. The Intraperitoneal Transcriptome of the Opportunistic Pathogen *Enterococcus faecalis* in Mice. PLOS ONE 10, e0126143. https://doi.org/10.1371/journal.pone.0126143

Neville, B.A., Forde, B.M., Claesson, M.J., Darby, T., Coghlan, A., Nally, K., Ross, R.P., O'Toole, P.W., 2012. Characterization of Pro-Inflammatory Flagellin Proteins Produced by *Lactobacillus ruminis* and Related Motile *Lactobacilli*. PLOS ONE 7, e40592. https://doi.org/10.1371/journal.pone.0040592

Paillet, T., Dugat-Bony, E., 2021. Bacteriophage ecology of fermented foods: anything new under the sun? Curr. Opin. Food Sci. 40, 102–111. https://doi.org/10.1016/j.cofs.2021.03.007

Philippe, C., Chaïb, A., Jaomanjaka, F., Claisse, O., Lucas, P.M., Samot, J., Cambillau, C., Le Marrec, C., 2021. Characterization of the First Virulent Phage Infecting *Oenococcus*

oeni, the Queen of the Cellars. Front. Microbiol. 11. https://doi.org/10.3389/fmicb.2020.596541

Saraoui, T., Parayre, S., Guernec, G., Loux, V., Montfort, J., Cam, A., Boudry, G., Jan, G., Falentin, H., 2013. A unique in vivo experimental approach reveals metabolic adaptation of the probiotic *Propionibacterium freudenreichii* to the colon environment. BMC Genomics 14, 911. https://doi.org/10.1186/1471-2164-14-911

Sprotte, S., Fagbemigun, O., Brinks, E., Cho, G.-S., Casey, E., Oguntoyinbo, F.A., Neve, H., Mahony, J., van Sinderen, D., Franz, C.M.A.P., 2022. Novel *Siphoviridae* phage PMBT4 belonging to the group b *Lactobacillus delbrueckii* subsp. *bulgaricus* phages. Virus Res. 308, 198635. https://doi.org/10.1016/j.virusres.2021.198635

Varet, H., Brillet-Guéguen, L., Coppée, J.-Y., Dillies, M.-A., 2016. SARTools: A DESeq2- and EdgeR-Based R Pipeline for Comprehensive Differential Analysis of RNA-Seq Data. PLOS ONE 11, e0157022. https://doi.org/10.1371/journal.pone.0157022

Weintraub, S.T., Redzuan, N.H.M., Barton, M.K., Amin, N.A., Desmond, M.I., Adams, L.E., Ali, B., Pardo, S., Molleur, D., Wu, W., Newcomb, W.W., Osier, M.V., Black, L.W., Steven, A.C., Thomas, J.A., 2019. Global Proteomic Profiling of *Salmonella* Infection by a Giant Phage. J. Virol. 93, 17. https://doi.org/10.1128/JVI.01833-18

Wick, R.R., Judd, L.M., Gorrie, C.L., Holt, K.E., 2017. Unicycler: Resolving bacterial genome assemblies from short and long sequencing reads. PLOS Comput. Biol. 13, e1005595. https://doi.org/10.1371/journal.pcbi.1005595

Wu, D., Yuan, Y., Liu, P., Wu, Y., Gao, M., 2014. Cellular responses in *Bacillus thuringiensis* CS33 during bacteriophage BtCS33 infection. J. Proteomics 101, 192–204. https://doi.org/10.1016/j.jprot.2014.02.016

Zhao, X., Chen, C., Shen, W., Huang, G., Le, S., Lu, S., Li, M., Zhao, Y., Wang, J., Rao, X., 2016. Global transcriptomic analysis of interactions between *Pseudomonas*

aeruginosa and bacteriophage PaP3. Sci. Rep. 6, 19237. https://doi.org/10.1038/srep19237

Tables:

Table 1: Number of down- or up-regulated genes for each comparison, fold change > 2 and < 0.5, p-value < 0.05.

Comparison	Level	Number of genes
T0 vs T15	up	0
	down	0
T0 vs T15P	up	45
	down	67
T15 vs T15P	up	36
	down	86
T0 vs T60	up	0
	down	1
T0 vs T60P	up	103
	down	147
T60 vs T60P	up	92
	down	123
T15 vs T60	up	0
	down	0
T15 vs T60P	up	95
	down	167
T15P vs T60	up	43
	down	42

746 T0 correspond to samples taken just before the infection with phage UCMA 21115. T15 and
747 T60 refers to 15 and 60 minutes after T0, respectively. P means that it is the infected
748 condition.

749

Figures captions:

Figure 1: Transmission electron micrographs of phage UCMA 21115.

Figure 2: Adsorption and one step growth curve of phage UCMA 21115 with *L. mali* UCMA 16447 in MRS broth at 30°C.

A. Adsorption of phage UCMA 21115 on *L. mali* 16447 during 30 minutes. **B.** One step growth curve of phage UCMA 21115 with *L. mali* UCMA 16447 during 300 minutes, where T0 is after 30 minutes of adsorption. Three independent experiments were carried out for each experiment and error bars indicate standard deviation.

Figure 3: Overview of the major functions of *L. mali* UCMA 16447 impacted during infection by phage UCMA 21115 at two time points by RNA-Seq analysis.

Bar graph displaying differentially expressed genes of *L. mali* UCMA 16447 during the infection by the phage UCMA 21115 at 15 (**A**) and 60 (**B**) minutes, respectively. Black bars indicate genes with an induced expression and white bars genes with a repressed expression in comparison to uninfected condition at the same time.

Figure 4: Simplified summary of principal functions with a level of expression induced (green) or repressed (red) in the transcriptomic study.

Figure 5: Embden-Meyerhof pathway of *L. mali* UCMA 16447 strain during infection by phage UCMA 21115, adapted from Muller *et al.,* 2015.

Genes impacted during the infection by phage UCMA 21115: repressed genes are mentioned in red and induced genes in green.

Figure 6: Number of differentially expressed proteins according to their functional classification during phage infection after 60 minutes of infection.

Comparison between T60 (60 min without phage) and T60P (60 min after phage infection). Black bars indicate proteins overexpressed and white bars proteins under expressed compared to uninfected condition.

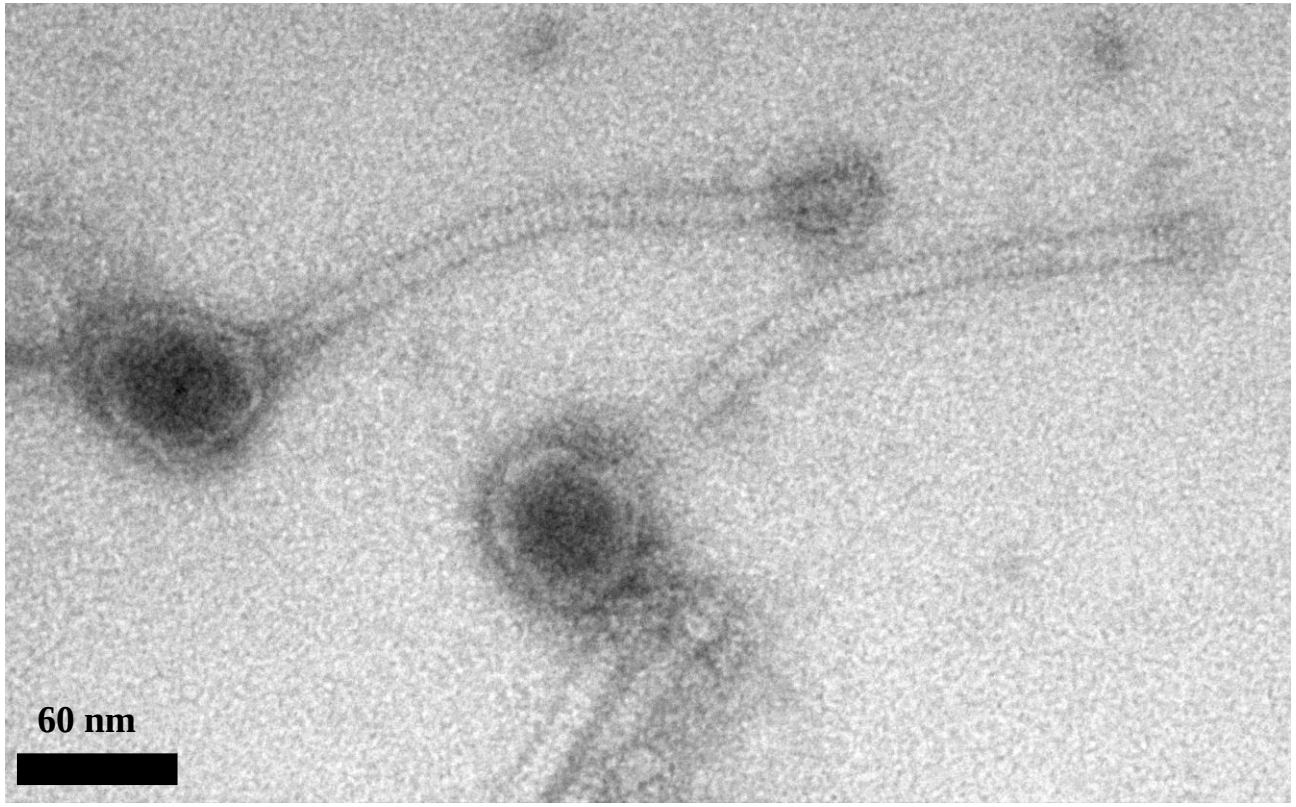
60 nm

A.

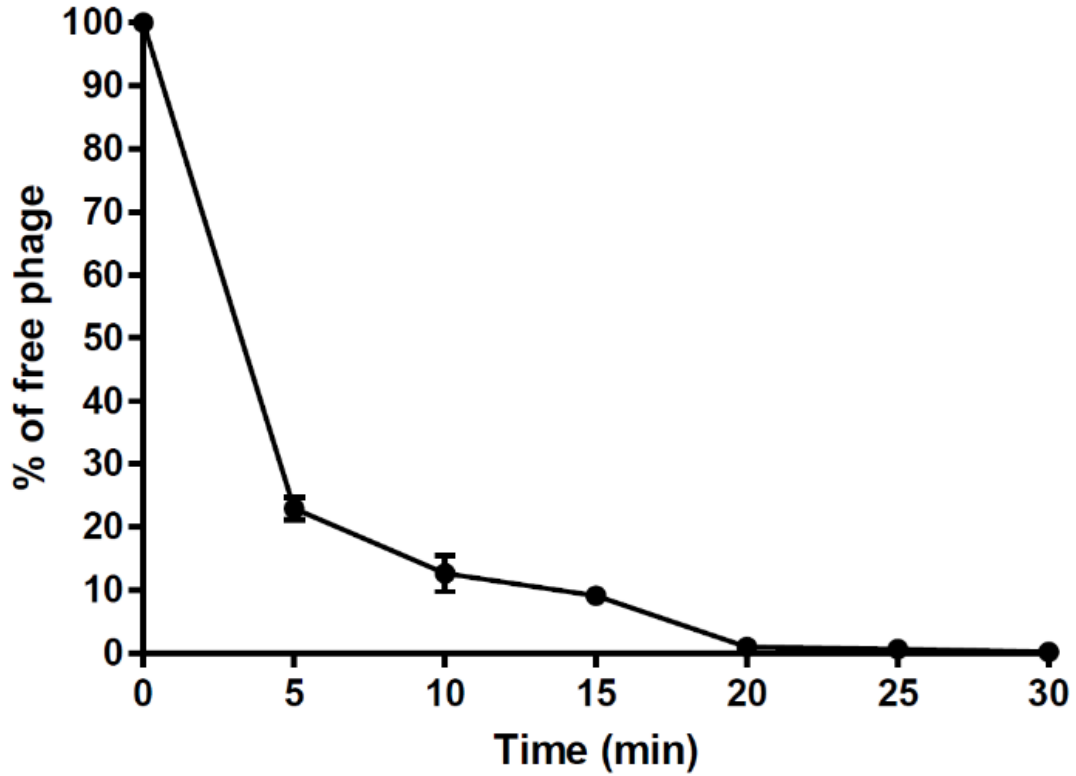
100
90
80
70
60
50
40
30
20
10
0
% of free phage
0
5
10
15
20
25
30
Time (min)

B.

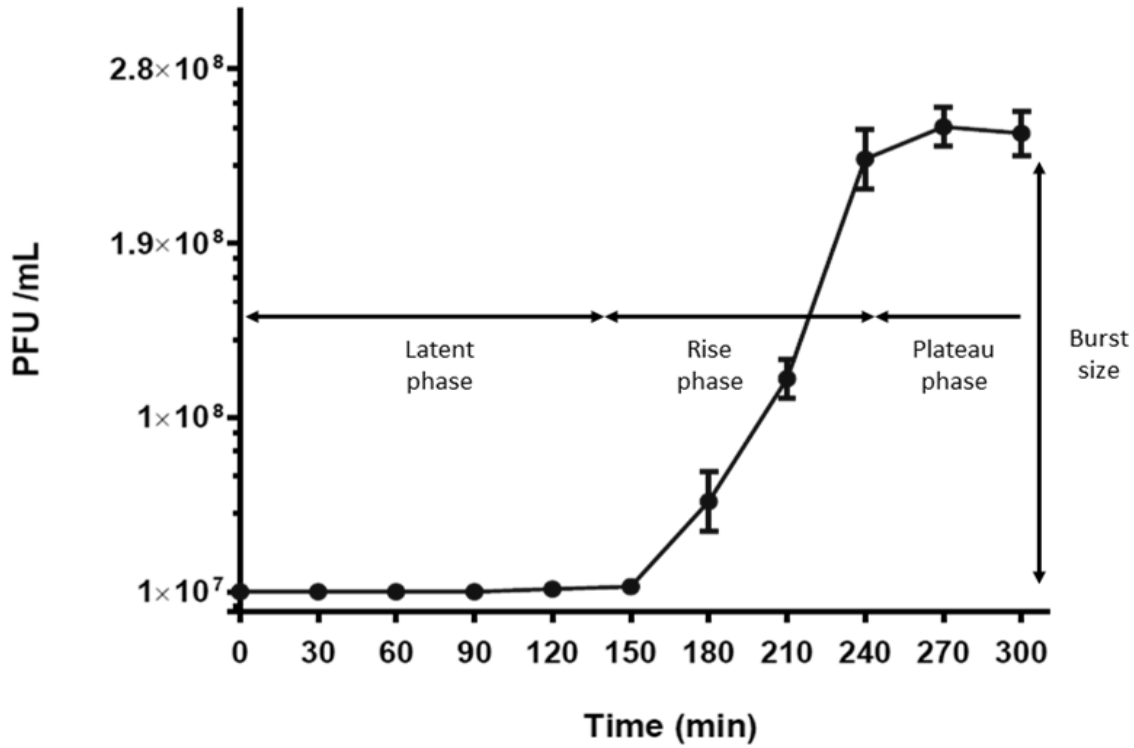
2.8×10⁸
1.9×10⁸
1×10⁸
1×10⁷
PFU /mL
Latent phase
Rise phase
Plateau phase
Burst size
0
30
60
90
120
150
180
210
240
270
300
Time (min)

A.

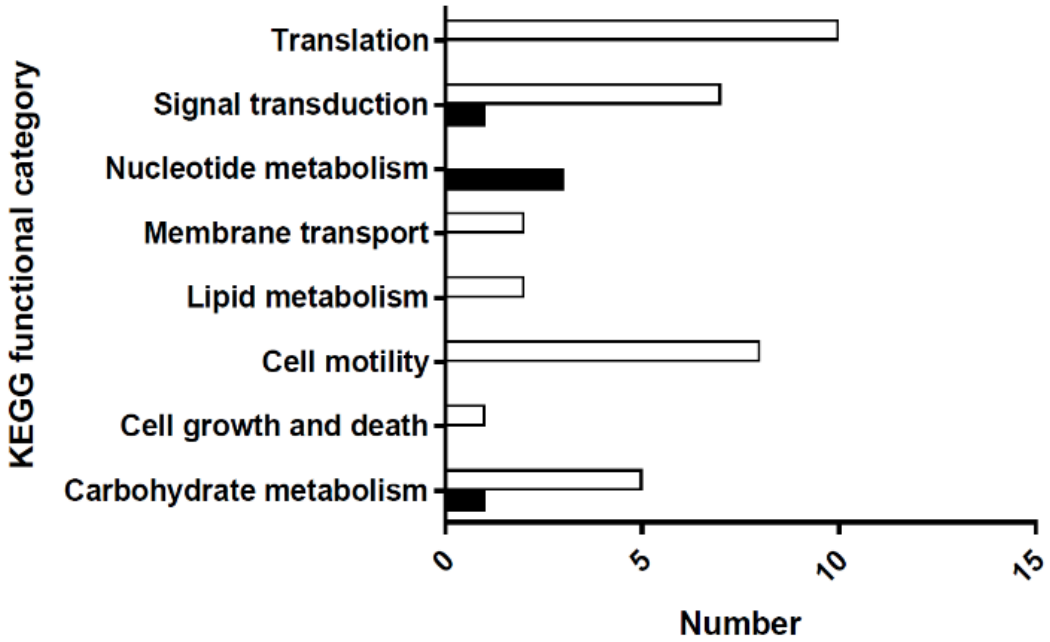
KEGG functional category
Translation
Signal transduction
Nucleotide metabolism
Membrane transport
Lipid metabolism
Cell motility
Cell growth and death
Carbohydrate metabolism
0
5
10
15
Number

B.

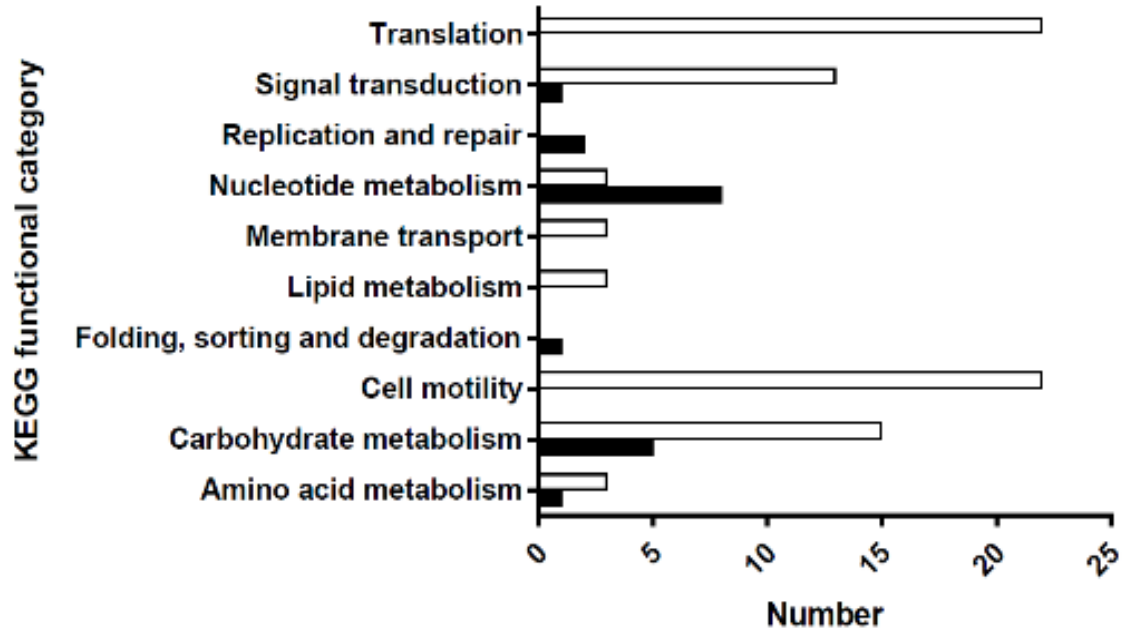
KEGG functional category
Translation
Signal transduction
Replication and repair
Nucleotide metabolism
Membrane transport
Lipid metabolism
Folding, sorting and degradation
Cell motility
Carbohydrate metabolism
Amino acid metabolism
0
5
10
15
20
25
Number

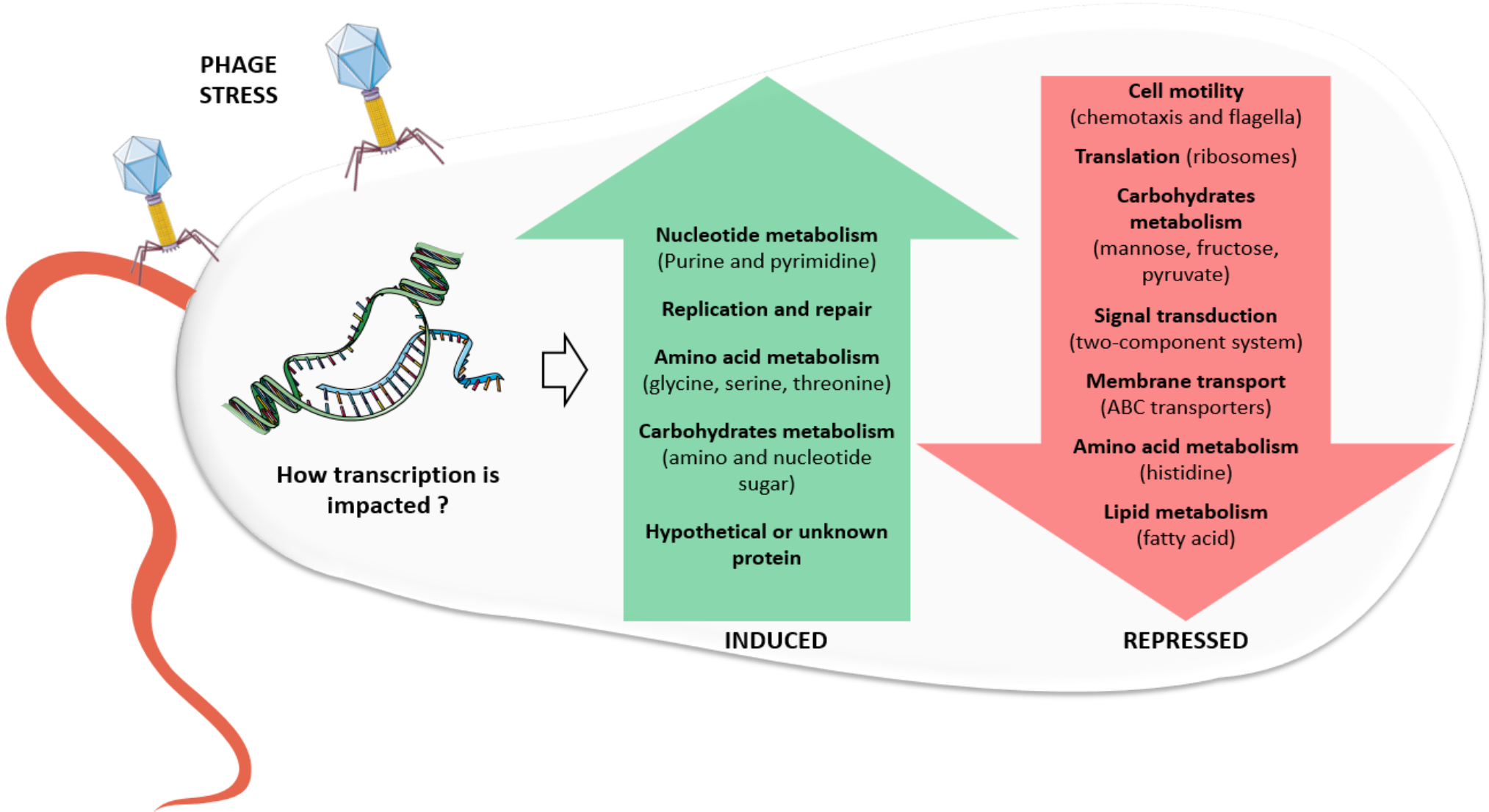
PHAGE
STRESS
How transcription is impacted ?
Nucleotide metabolism (Purine and pyrimidine)
Replication and repair
Amino acid metabolism (glycine, serine, threonine)
Carbohydrates metabolism (amino and nucleotide sugar)
Hypothetical or unknown protein
INDUCED
Cell motility (chemotaxis and flagella)
Translation (ribosomes)
Carbohydrates metabolism (mannose, fructose, pyruvate)
Signal transduction (two-component system)
Membrane transport (ABC transporters)
Amino acid metabolism (histidine)
Lipid metabolism (fatty acid)
REPRESSED

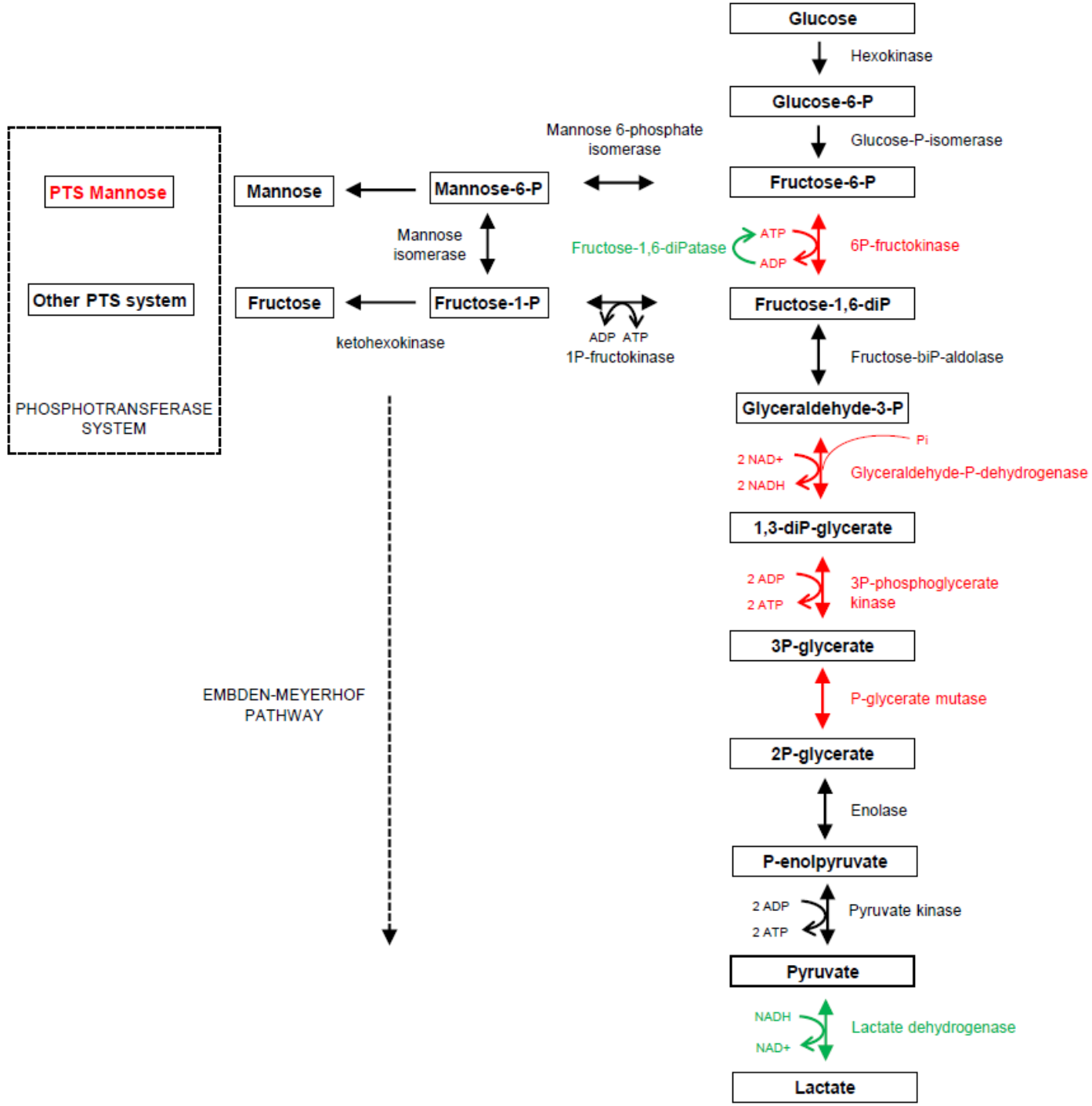
Glucose
Hexokinase
Glucose-6-P
Glucose-P-isomerase
Fructose-6-P
Mannose 6-phosphate isomerase
PTS Mannose
Mannose
Mannose-6-P
Mannose isomerase
Other PTS system
Fructose
Fructose-1-P
ketohexokinase
Fructose-1,6-diPatase
ATP
ADP
6P-fructokinase
ADP ATP
1P-fructokinase
Fructose-1,6-diP
Fructose-biP-aldolase
PHOSPHOTRANSFERASE SYSTEM
Glyceraldehyde-3-P
Pi
2 NAD+
2 NADH
Glyceraldehyde-P-dehydrogenase
1,3-diP-glycerate
2 ADP
2 ATP
3P-phosphoglycerate kinase
3P-glycerate
P-glycerate mutase
EMBDEN-MEYERHOF PATHWAY
2P-glycerate
Enolase
P-enolpyruvate
2 ADP
2 ATP
Pyruvate kinase
Pyruvate
NADH
NAD+
Lactate dehydrogenase
Lactate

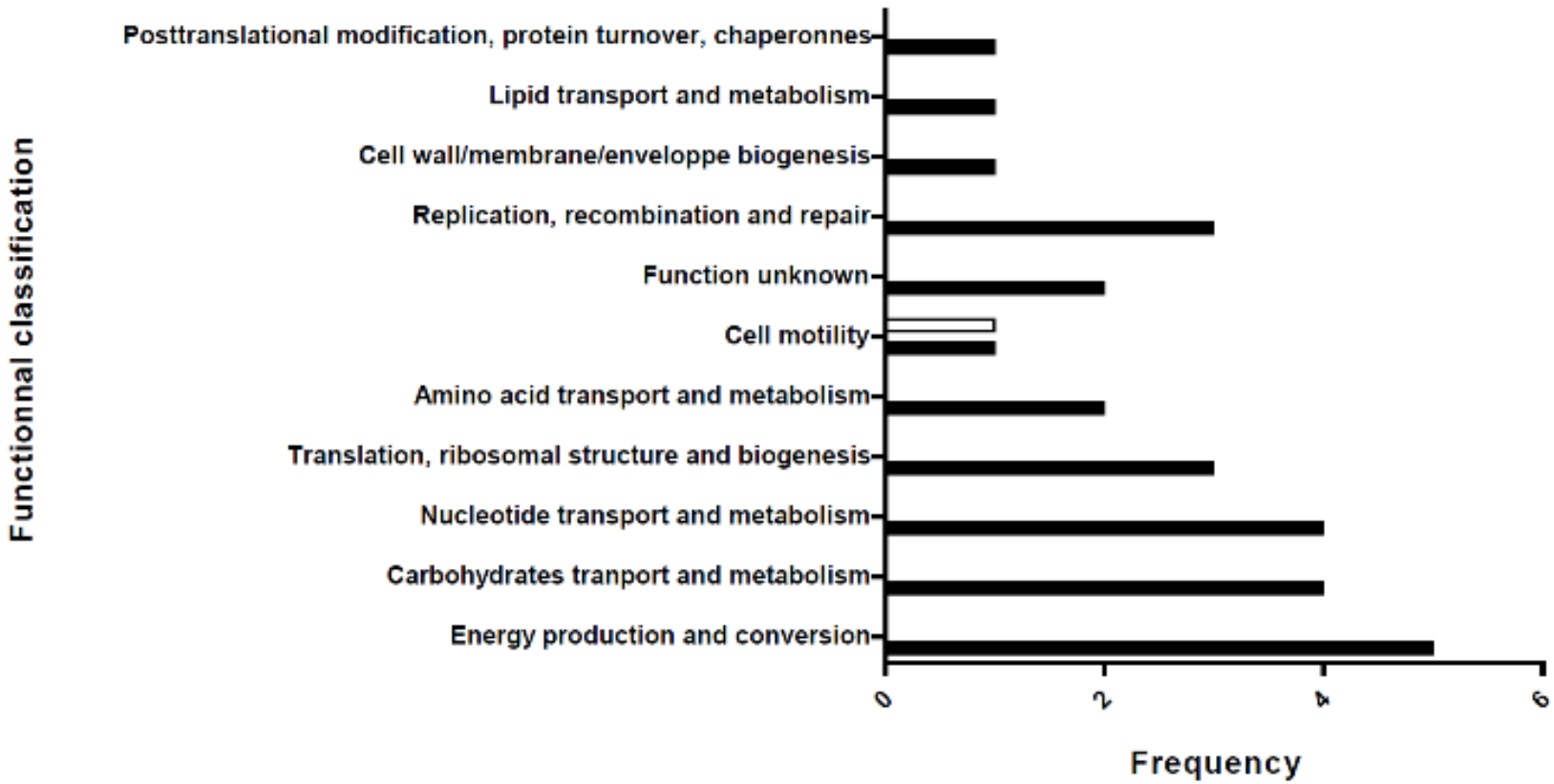
Functionnal classification
Posttranslational modification, protein turnover, chaperonnes
Lipid transport and metabolism
Cell wall/membrane/enveloppe biogenesis
Replication, recombination and repair
Function unknown
Cell motility
Amino acid transport and metabolism
Translation, ribosomal structure and biogenesis
Nucleotide transport and metabolism
Carbohydrates tranport and metabolism
Energy production and conversion
0
2
4
6
Frequency